JOURNAL OF MATERIALS SCIENCE 29 (1994) 4260–4267

Plasma-enhanced fluorination of $YBa_2Cu_3O_{7-\delta}$ ceramics

Part II *Interaction mechanisms between the reactive species and the materials*

C.MAGRO, A. TRESSAUD, N. HUDÁKOVÁ*, J. ETOURNEAU
Laboratoire de Chimie du Solide du CNRS, Université de Bordeaux I, 351, cours de la Libération, 33405 Talence Cedex, France

C. CARDINAUD, G. TURBAN
Institut des Matériaux de Nantes, 2 rue de la Houssinière, 44072 Nantes Cedex 03, France

Mechanisms of interaction between the reactive species of a $(CF_4 + O_2)$ plasma and $YBa_2Cu_3O_{7-\delta}$ ceramics have been proposed through detailed angle-resolved X-ray photoelectron spectroscopic analyses. At the surface of the outer grains, the plasma treatment removes $(OH)^-$ and $(CO_3)^{2-}$ species contained in the degradation layer and gives rise to a fluoride-rich layer, whereas in the bulk of the material the occurrence of metal–fluorine bonds in the superconducting phase has been assumed. An increase of the oxidation state of copper has been also detected, confirming the oxidizing effect of the plasma treatment. A comparison with the oxidation mechanisms obtained by fluorine gas treatment is proposed.

1. Introduction

In a previous paper (Part I) [1], a new surface treatment of high T_c superconductors has been proposed: plasma-enhanced fluorination (PEF). By means of this technique the "Cu^{3+}" content and the critical current density of $YBa_2Cu_3O_{7-\delta}$ ceramics are simultaneously improved. This paper is devoted to the investigation of the interaction between the reactive species of a $(CF_4 + O_2)$ plasma and the surface of the $YBa_2Cu_3O_{7-\delta}$ ceramics through detailed angle-resolved X-ray photoelectron spectroscopic analyses. The results will be compared with those obtained on ceramics heated under fluorine-gas.

2. Experimental procedure

The preparation of $YBa_2Cu_3O_{7-\delta}$ ceramics and the description of the plasma equipment were detailed in Part I [1]. The ceramics were obtained by means of a solid-state sintering procedure. The microstructure and the compositional homogeneity of the samples were determined by both scanning electronic microscopy and electron microprobe analysis. The plasma experiments were carried out in a barrel-type apparatus. The gas used was a mixture of CF_4 and O_2 excited by a radiofrequency source at 13.56 MHz. The influence of the various experimental parameters on the resulting superconducting properties of the samples was systematically investigated. The conditions of PEF treatment giving rise to optimized superconducting properties (i.e. improvement of both critical temperature and critical current density) were found to be mainly related to three parameters:

(i) the nature of the reactive medium, the optimized composition of which corresponded to an addition of 25%O_2 to a CF_4 plasma;

(ii) the total pressure, p, lower than 10^{-4} bar;

(iii) the reaction time of about 30 min at a temperature lower than 100 °C.

Some quantitative results of the improvement of the superconducting properties of $YBa_2Cu_3O_{7-\delta}$ ceramics by PEF treatment have been given in Table V of Part I [1].

On the other hand, conventional F_2-gas treatment was performed below 100 °C in a pure fluorine atmosphere for several hours. It has been shown that this type of surface treatment was efficient for protecting $YBa_2Cu_3O_{7-\delta}$ ceramics against moist air by forming a fluorinated layer about 30 nm thick at the grain boundaries [2]. The critical current density of the fluorine-gas treated material was likewise improved.

After PEF of fluorine-gas treatments, the ceramics were characterized by several complementary techniques.

(a) Chemical analysis by Mohr-salt titration, to determine the "Cu^{3+}" content in the sample.

(b) Electron microprobe analysis (EMPA) performed on polished surfaces of fractures of the sintered pellets, in order to determine the distribution of fluorine in the bulk of the ceramics; standard samples used were $YBa_2Cu_3O_{7-\delta}$ and BaF_2 crystals.

(c) Auger electron spectroscopy (AES) using a scanning Auger electronic microscope. The thickness of the

* *Permanent address*: Institute of Experimental Physics, Slovak Academy of Sciences, Watsonova 47, 04353 Košice, Slovakia.

0022–2461

fluorinated layer was determined by examining the fluorine concentration profile by erasing step by step the sample with the help of argon ion sputtering. The analysed depth was around 2 nm for every step.

(d) Angle-resolved X-ray photoelectron spectroscopy (XPS), using a Leybold AG LH 12 type spectrometer equipped with a monochromator.

Two different types of information could be drawn from these experiments. The first one concerned the interaction of the reactive species (F_2 or F^*) with the grains at the surface of the pellets. In this case the data were obtained from freshly prepared pellets. The other one dealt with the interaction between the reactive species and the surface of the inner grains of the pellets, the information being obtained from the centre of polished fractures. In every case, a surface of several square millimetres was analysed, and the involved depth, d, depended on the electron emergence angle, θ, of the X-ray beam with respect to the perpendicular of the surface of the sample (if $\theta = 0°$, then $d \approx 8$ nm and if $\theta = 60°$, then $d \approx 4$ nm). Angle-resolved measurements were also performed for intermediate angles between 0° and 60°. During the experiment, copper was partly reduced to monovalent species; this X-ray photoreduction phenomenon has already been observed in copper-based superconductors [3]. This behaviour prevents further interpretation on the oxidation state of copper. Therefore, the XPS study was carried out on the Y 3d, Ba $3d_{5/2}$, Ba 4d, O 1s, F 1s and C 1s levels, respectively. Because the pellets are held by gilt screws, peaks related to the Au $4s_{5/2}$ contribution are observed.

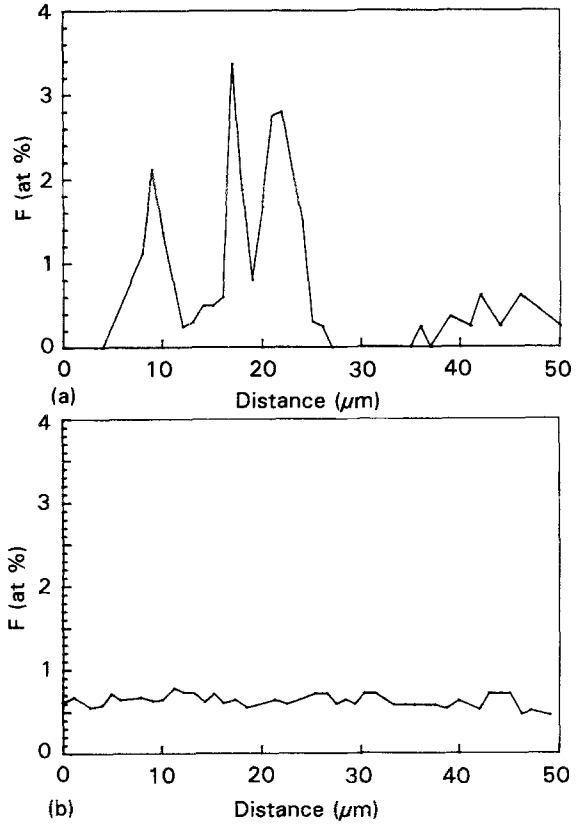

Figure 1 Fluorine concentration profiles determined by EMPA in the bulk of $YBa_2Cu_3O_{7-\delta}$ ceramics fluorinated by (a) fluorine gas and (b) PEF treatments.

3. Distribution of fluorine inside the $YBa_2Cu_3O_{7-\delta}$ ceramic after fluorine-gas and PEF treatments

Fluorine-content profiles have been obtained by EMPA on the polished surface of a fracture of fluorinated pellets. Profiles were carried out along 50 μm in the central part of the fracture. These profiles depend on the used fluorination treatment as shown in Fig. 1. In the case of fluorine-gas treatment, the fluorine distribution appears to be inhomogeneous, the fluorine atomic percentage fluctuating between 0% and 3%. On the contrary, the PEF treatment leads to an homogeneous distribution of fluorine around 0.5% in the bulk of the ceramic.

X-ray maps of fluorine were also performed to locate more precisely this element inside the materials (Fig. 2). For a fluorine-gas treated sample, fluorine is mainly located at the pore–grain interfaces, as shown by the good agreement between the pore location observed by SEM and the fluorine location (Fig. 2a). On the other hand, a smaller quantity of fluorine is present homogeneously in the bulk of the PEF-treated ceramic (Fig. 2b).

4. Angle-resolved X-ray photoelectron spectroscopic analyses of fluorinated $YBa_2Cu_3O_{7-\delta}$ ceramics

4.1. Interaction of the reactive fluorinated species with the surface of outer grains of the $YBa_2Cu_3O_{7-\delta}$ ceramics

As shown in Fig. 3a, all Y and Ba XPS spectra of $YBa_2Cu_3O_{7-\delta}$ ceramics are currently characterized before fluorination by two types of contributions. For one type, the binding energies, E_b, are strongly shifted towards lower values. These so-called "superconducting peaks" are attributed to metal–oxygen bonds corresponding to the $YBa_2Cu_3O_{7-\delta}$ lattice [4]. The second type of contribution corresponds to the degradation layer (Y–OH and Ba–CO_3 bonds) [5].

4.1.1. Fluorine gas treatment

As shown in Fig. 3b, peaks corresponding to both superconducting phase and degradation layer have disappeared. Two types of contribution are now observed, which are both shifted towards higher binding energy.

For the first type of contribution the binding energies are slightly shifted towards higher E_b. The corresponding energies are 158.9 eV (Y 3d), 780.2 eV (Ba $3d_{5/2}$) and 90.0 eV (Ba 4d). These contributions can be unambiguously attributed to metal–fluorine bonds which are formed during the fluorination process and which are similar to those observed in binary compounds YF_3 or BaF_2 [5]. These observations are in good agreement with the low binding-energy contribution observed at 684.7 eV in the F 1s spectra and assigned to fluorine–metal bonds (Fig. 4). The F 1s envelope consists of two additional contributions related to the interaction of the reactive fluorospecies with the degradation layer. The high-energy component located at 689.8 eV can be currently associated

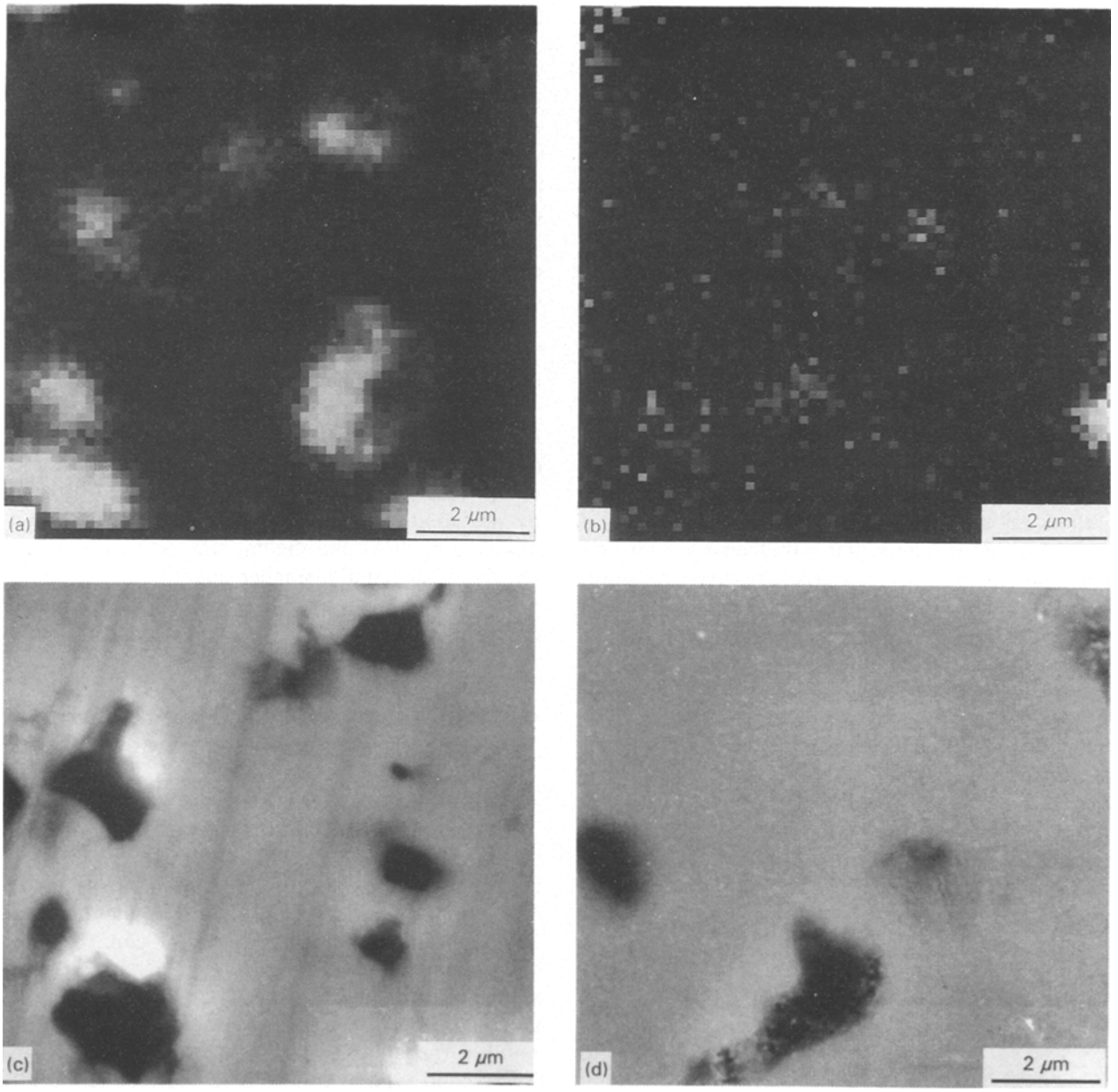

Figure 2 (a, b) X-ray maps of fluorine and (c, d) scanning electron micrographs of samples fluorinated by (a, c) fluorine gas and (b, d) PEF treatments.

with covalent fluorine–carbon bonds as found in graphite fluorides, $(CF)_n$ for example [6]. This observation is supported by a C 1s peak at 288.3 eV as seen in Fig. 5. The other type of contribution, located at 686.3 eV, is the most intense one. Although it seems hazardous to raise definitive conclusions on the nature of these species, the similarity of the experimental E_b values with those observed for HF_2^--based graphite intercalation compounds should be noted [6]. The formation of the $(CF)_n$ and HF_2^- species may be due to the decomposition by fluorine-gas of the degradation layer which is mainly composed of carbonate and hydroxyl groups.

The second type of contribution exhibits binding energies strongly shifted towards higher E_b. These energies are, respectively, 162.0 eV (Y 3d), 783.5 eV (Ba $3d_{5/2}$), and 92.2 eV (Ba 4d). The corresponding metal–fluorine bonds appear to be even more ionic than those observed in the binary fluorides (YF_3 or BaF_2). This observation could be explained starting from the competition between Cu–F and Y–(or Ba–)F bonds due to the inductive effect [7]: the increase of the ionicity of both Y–(or Ba–)F bonds, reflected by a shift of the core levels energy of yttrium and barium towards the higher energy, results from the enhancement of the covalency of the Cu–F bond. This effect can be ascribed to a partial oxidation of Cu(II) into Cu(III) during the fluorination process.

In order to examine how the intensity of the peaks corresponding to the levels energies of yttrium, barium and oxygen atoms vary qualitatively, angle-resolved measurements have been performed as a function of the electron emergence angle, θ, of the X-ray beam between 0° and 60°. As shown in Fig. 5, the relative intensity of the higher energy peaks is smaller as the analysed depth becomes greater, suggesting that the Cu(III) concentration gradient decreases from the surface to the bulk. This observation is also

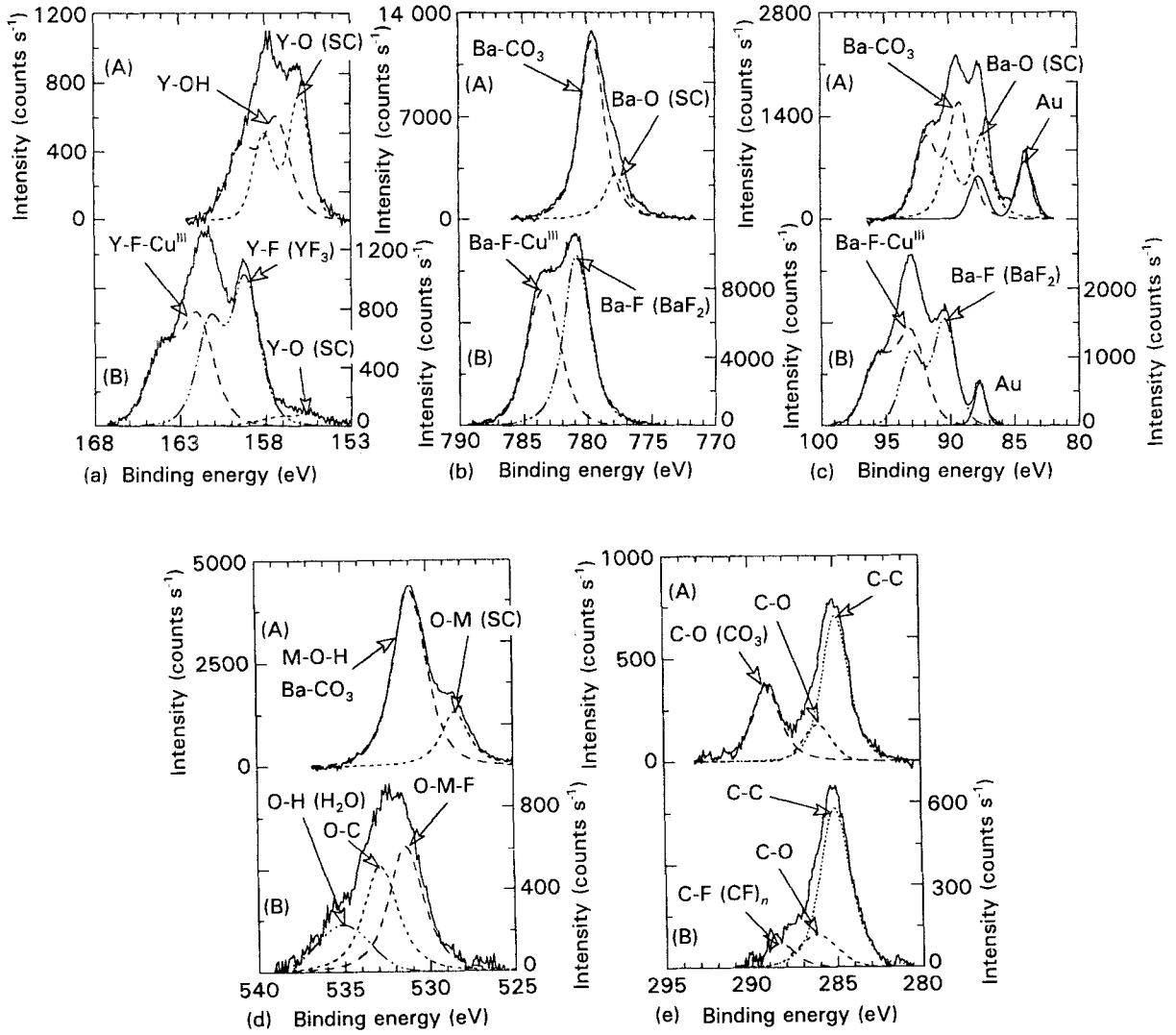

Figure 3 (a) Y 3d, (b) Ba $3d_{5/2}$, (c) Ba 4d, (d) O 1s and (e) C 1s emission spectra obtained at the surface of the outer grains of the $YBa_2Cu_3O_{7-\delta}$ ceramics ($\theta = 0°$) (A) before and (B) after fluorine gas treatment ($T_{F_2} = 100\,°C$; the superconducting peaks of the phase are noted SC).

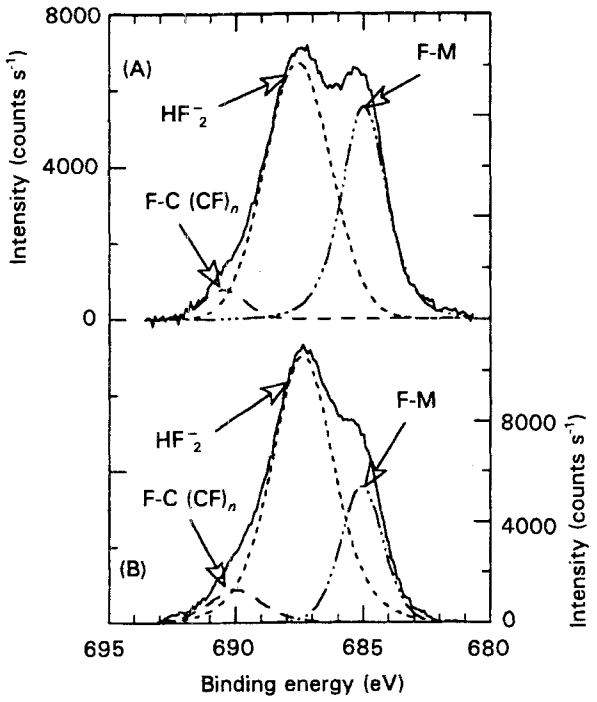

Figure 4 F 1s emission spectra obtained from angle-resolved analyses: (A) $\theta = 0°$, and (B) $\theta = 60°$, at the surface of the outer grains of the fluorine gas treated $YBa_2Cu_3O_{7-\delta}$ ceramics ($T_{F_2} = 100\,°C$).

corroborated by the examination of the intensity of the oxygen 1s level corresponding to oxyfluorinated species, which increases with increasing analysed depth (Fig. 5). All the results suggest that the layer (≈ 30 nm thick) obtained after fluorine gas treatment of the $YBa_2Cu_3O_{7-\delta}$ ceramic is likely composed of an oxyfluoride as major phase, whose oxygen content increases with increasing depth, whereas the Cu(III) content decreases.

By comparison with the energy of the peaks corresponding to the superconducting phase, the energy shift of these peaks after fluorine gas treatment is much too high to consider that the oxyfluoride can be derived from the $YBa_2Cu_3O_{7-\delta}$ compound.

4.1.2. Plasma-enhanced (PEF) treatment

As shown in Fig. 6, for yttrium and barium elements, both peaks corresponding to the component of the superconducting phase and to the degradation layer have disappeared after the PEF treatment. New distinct peaks are now observed at 158.9 eV (Y 3d), 780.2 eV (Ba $3d_{5/2}$) and 90.0 eV (Ba 4d). They can be unambiguously ascribed to metal–fluorine bonds already discussed in the case of the fluorine gas treatment. These observations are supported by a unique

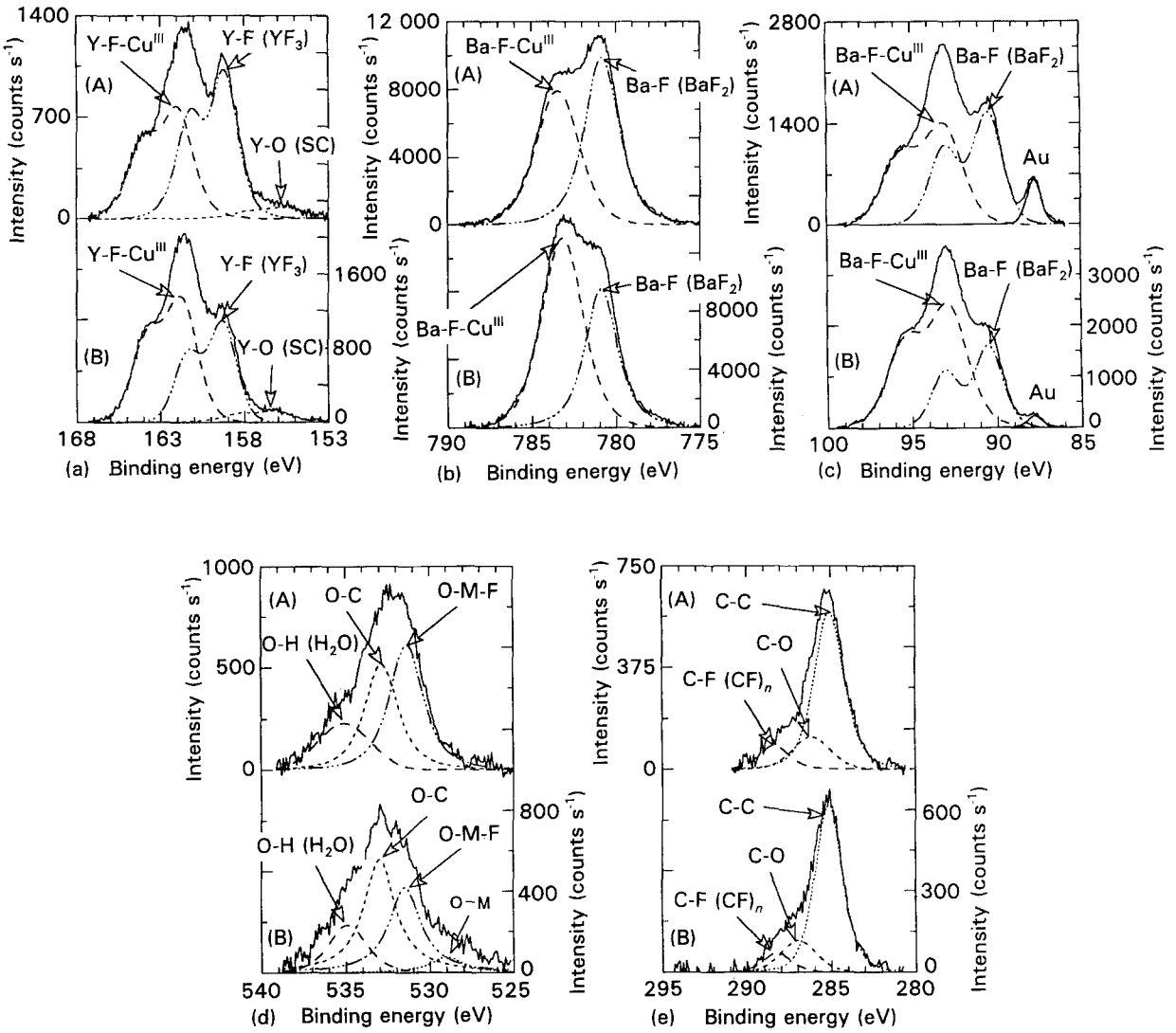

Figure 5 (a) Y 3d, (b) Ba $3d_{5/2}$, (c) Ba 4d, (d) O 1s and (e) C 1s emission spectra obtained from angle-resolved analyses: (A) $\theta = 0°$, and (B) $\theta = 60°$, at the surface of the outer grains of fluorinated $YBa_2Cu_3O_{7-\delta}$ ceramics ($T_{F_2} = 100\,°C$).

F 1s peak at 684.7 eV corresponding to fluorine–metal bonds (Fig. 7). Contrary to the fluorine gas treatment, the PEF process removes the $(OH)^-$ and $(CO_3)^{2-}$ species without the $(CF)_n$ and HF_2^- species described in Fig. 4. The interaction of the F^* species with the degradation layer could lead to the formation of volatile compounds such as COF or COF_2.

A fluorinated layer is substituted for the degradation layer; its thickness had been evaluated to be around 7 nm thick by Auger electron spectroscopy for a PEF-treated $YBa_2Cu_3O_{7-\delta}$ single crystal. Moreover, its composition is more homogeneous than that obtained from a fluorine gas treatment; it seems actually to consist mostly of fluorides and does not exhibit higher E_b contributions, which has been attributed to M–F–Cu(III) bonds in the case of a fluorine gas treatment. In the O 1s spectrum the intensity of the peaks corresponding to oxyfluorinated species at 531.4 eV does not depend on the analysed depth.

4.2. Interaction of reactive fluorinated species with the surface of inner grains of $YBa_2Cu_3O_{7-\delta}$ ceramics

4.2.1. Fluorine-gas treatment

The XPS spectra are similar to those observed at the surface of the outer grains of the materials, i.e. as those of Figs 3–5. These results suggest that the fluorine gas treatment removes the degradation layer even in the bulk of the ceramics to form a fluorinated layer protecting the materials against moist air (H_2O and CO_2).

4.2.2. PEF treatment

As shown in Fig. 8, after the PEF treatment the peaks corresponding in the Y 3d, Ba $3d_{5/2}$ and Ba 4d spectra to the superconducting component and to the degradation layer remain unchanged, and no new peak appears in the high E_b range. These observations suggest that the PEF treatment does not decompose either the degradation layer or the superconducting phase at the surface of the inner grains, as observed for fluorine-gas fluorination. Unfortunately, the fluorine content, distributed homogeneously in the sample as shown in Fig. 2b and previously determined by EMPA to be around 0.5 at%, is too small to be detected by XPS.

In addition, it can be pointed out that the peaks corresponding to the components of the superconducting phase are slightly shifted towards higher binding energy (+ 0.2 eV) as shown in Fig. 9. These displacements cannot be attributed to a charge effect, because

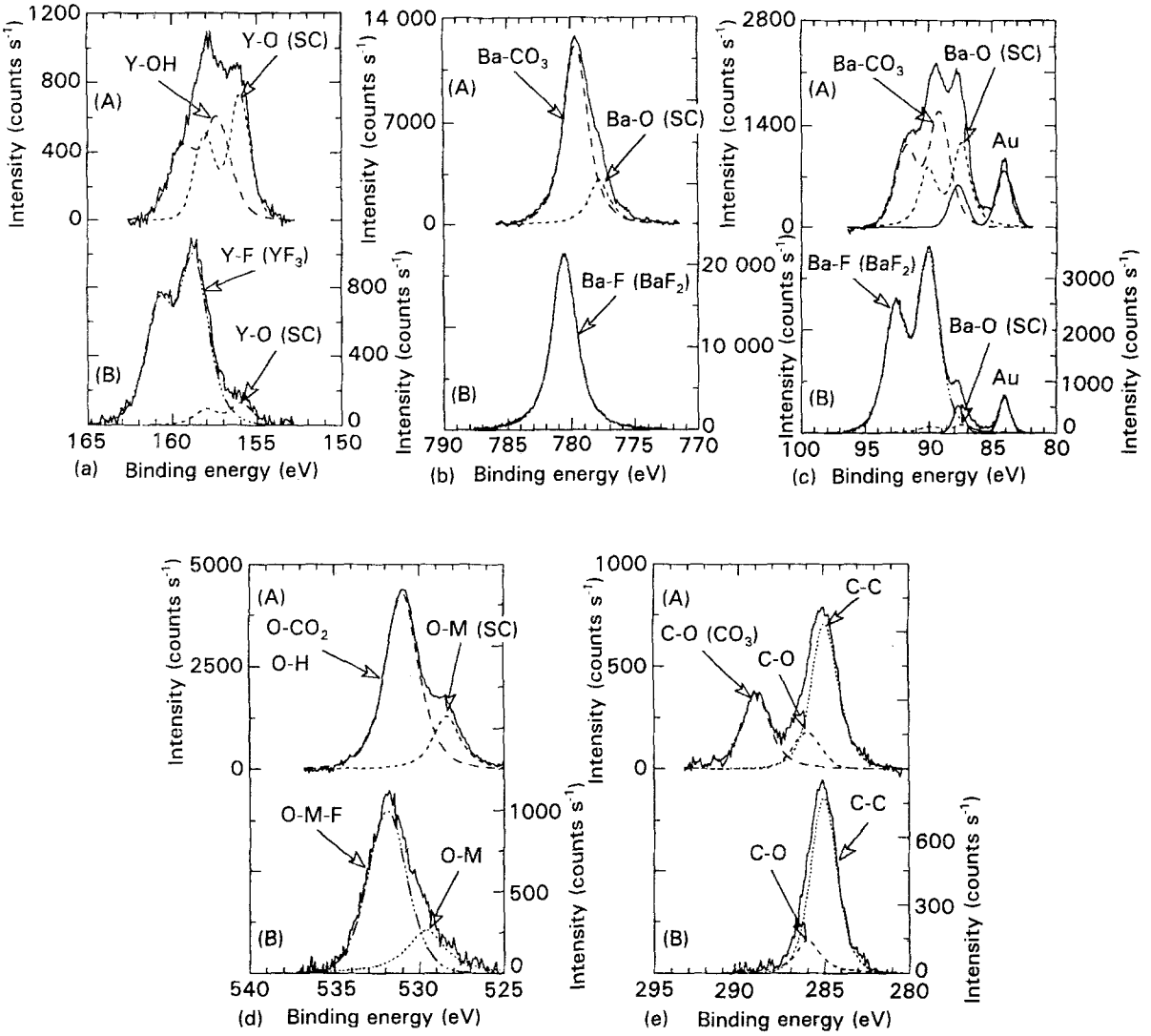

Figure 6 (a) Y 3d, (b) Ba $3d_{5/2}$, (c) Ba 4d, (d) O 1s and (e) C 1s emission spectra obtained at the surface ($\theta = 0°$) of the outer grains of the $YBa_2Cu_3O_{7-\delta}$ ceramics (A) before, and (B) after the $CF_4 + 25\%O_2$ plasma treatment (the peaks of the superconducting phase are noted SC).

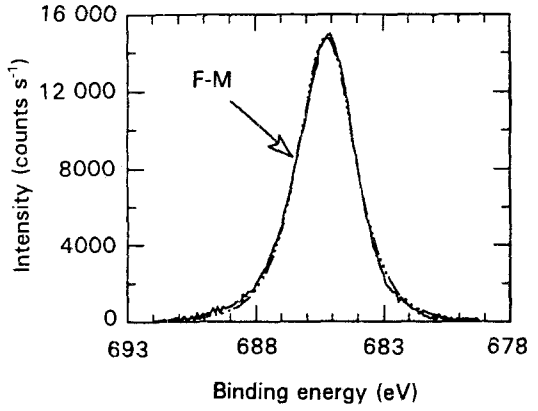

Figure 7 F 1s emission spectra obtained on the surface ($\theta = 0°$) of the outer grains of the $YBa_2Cu_3O_{7-\delta}$ ceramics treated by a $CF_4 + 25\%O_2$ plasma.

the peaks corresponding to the degradation layer remain unchanged. Therefore, the following assumption can be launched for explaining the Y 3d and Ba $3d_{5/2}$ spectra (Fig. 9a, b): metal–fluorine bonds would be present inside the superconducting phase; the slight shift observed (≈ 0.2 eV) towards higher energies for the peaks Y 3d, Ba $3d_{5/2}$ and Ba 4d, corresponding to the component of the superconducting phase, is due therefore to an increase of the ionicity of the corresponding bonds.

However, the enhancement of the ionicity of these bonds may also result from an increase of the covalency of the competitive Cu–O bonds (Fig. 9c), due to an increase of the concentration of Cu(III). This observation is corroborated by Mohr-salt titrations as shown in Table I of Part I [1]. From these results it seems obvious that both the anionic non-stoichiometry and Cu^{3+} content are affected by the oxidizing effect of fluorine. A similar change in binding energy of core levels of yttrium and barium has already been observed on $YBa_2Cu_3O_{7-\delta}$ treated under oxygen [8], in which an increase of Cu(III) occurs.

5. Conclusion

The interaction of reactive species (F_2 and F^*) with the surface of both outer and inner grains of $YBa_2Cu_3O_{7-\delta}$ ceramics have been investigated. The fluorine-gas treatment removes similarly $(OH)^-$ and $(CO_3)^{2-}$ species located in the degradation layer of the surface of both outer and inner grains of the materials, and also leads to the formation of HF_2^- and $(CF)_n$

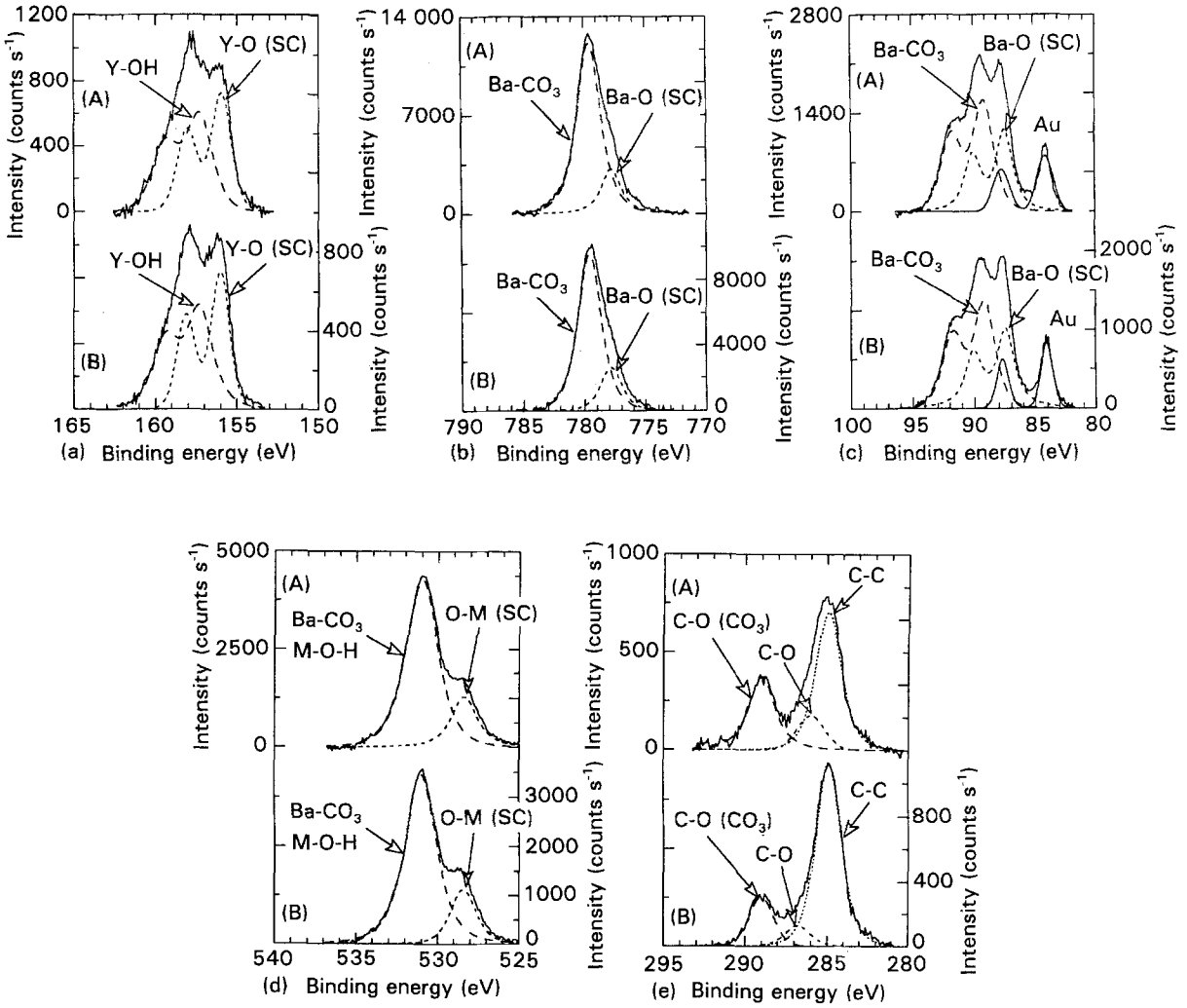

Figure 8 (a) Y 3d, (b) Ba $3d_{5/2}$, (c) Ba 4d, (d) O 1s and (e) C 1s emission spectra obtained at the surface ($\theta = 0°$) of the inner grains of the $YBa_2Cu_3O_{7-\delta}$ ceramics (A) before, and (B) after the $CF_4 + 25\%O_2$ plasma treatment (the peaks of the superconducting phase are noted SC).

species as observed in the F 1s spectra. The fluorination process gives rise at the surface of the grains to the formation of a fluorinated layer about 30 nm thick and containing a concentration gradient of Cu(III) and oxyfluorinated species. This layer efficiently protects the $YBa_2Cu_3O_{7-\delta}$ ceramics against moist air and the superconducting properties are also improved. The PEF treatment removes the $(OH)^-$ and $(CO_3)^{2-}$ species from in the degradation layer of outer grains of the materials, without forming $(CF)_n$ and HF_2^- species. The fluorination process gives rise to an homogeneously fluorinated layer, about 7 nm thick at the surface of the outer grains of the materials. On the other hand, the PEF treatment does not seem to

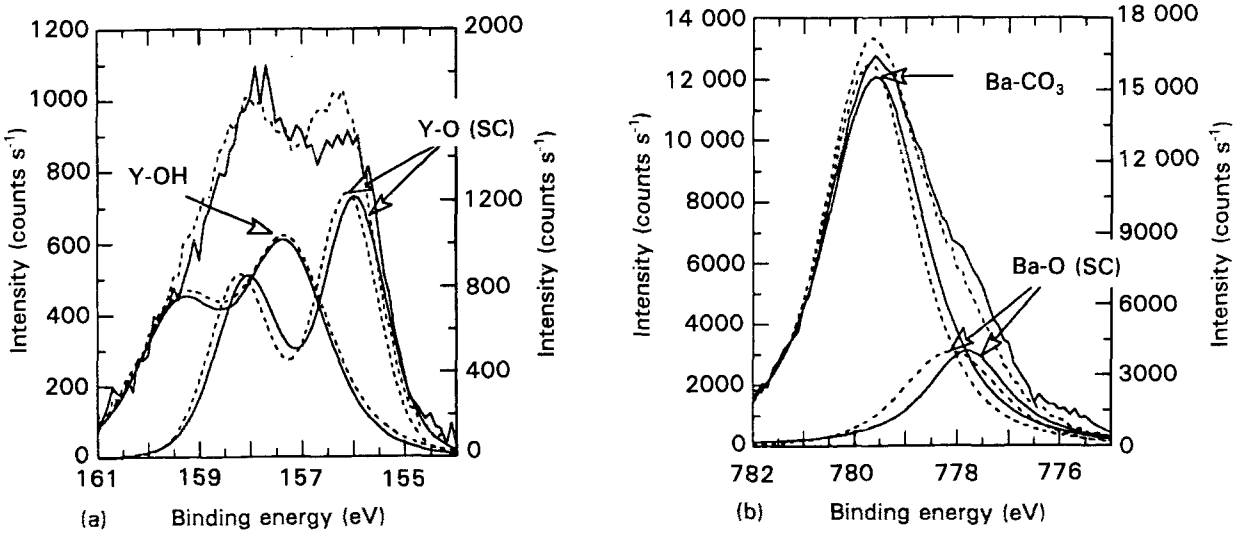

Figure 9 (a) Y 3d, (b) Ba $3d_{5/2}$, and (c) O 1s emission spectra obtained at the surface ($\theta = 0°$) of the inner grains of the $YBa_2Cu_3O_{7-\delta}$ (——) before and (– – –) after the $CF_4 + 25\%O_2$ plasma treatment (the peaks of the superconducting phase are noted SC).

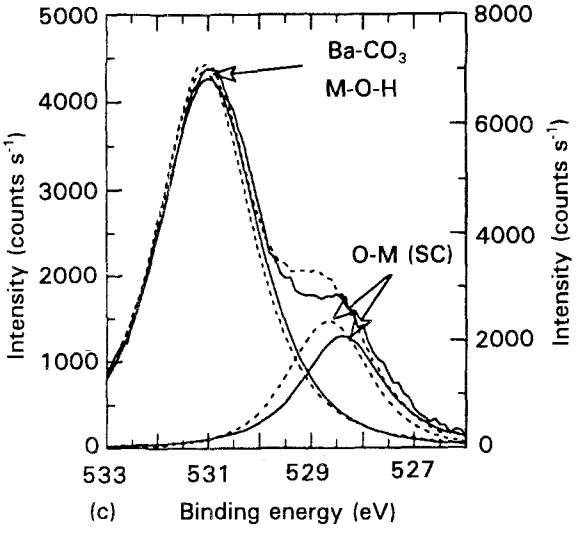

produce a fluorine-rich layer at the surface of inner grains of the materials, but would rather lead to the formation of metal–fluorine bonds inside the superconducting phase due to an oxidation process by $F^{\bullet}$ species.

Acknowledgements

The authors thank B. Chevalier for valuable suggestions, L. Lozano for fluorination experiments and M. Lahaye for EMPA investigations. This work was carried out as a part of a CNRS research programme on superconductors with the support of Rhône–Poulenc Recherche.

References

1. C. MAGRO, A. TRESSAUD, N. HUDAKOVA, L. LOZANO, C. CARDINAUD and G. TURBAN, *J. Mater. Sci.* **29** (1994) in press.
2. A. TRESSAUD, B. CHEVALIER, B. LEPINE, J. M. DANCE, L. LOZANO, J. GRANNEC, J. ETOURNEAU, R. TOURNIER, A. SULPICE and P. LEJAY, *Mod. Phys. Lett.* **B2** (1988) 1183.
3. W. HERZOG, M. SCHWARZ, H. SIXL and R. HOPPE, *Z. Phys.* **B71** (1988) 19.
4. S. MYHRA, J. C. RIVIERE, A. M. STEWARD and P. C. HEALY, *ibid.* **B72** (1988) 413.
5. R. P. VASQUEZ, M. C. FOOTE and B. D. HUNT, *J. Appl. Phys.* **66** (1989) 4866.
6. H. TOUHARA, Y. GOTO, N. WATANABE, K. IMAEDA, T. ENOKI, H. INOKUCHI and Y. MIZUTANI, *Synth. Met.* **23** (1988) 461.
7. J. ETOURNEAU, J. PORTIER and F. MENIL, *J. Alloys Compounds* **188** (1992) 1.
8. P. C. HEALY, S. MYHRA and A. M. STEWARD, *Philos. Mag.* **B58** (1988) 257.

Received 4 May
and accepted 29 October 1993